Salmonella enterica genomes from victims of a major 16th century epidemic in Mexico

Authors: Åshild J. Vågene[1,2#], Alexander Herbig[1,2#]*, Michael G. Campana[2, 3]†, Nelly M. Robles García[4], Christina Warinner[1], Susanna Sabin[1], Maria A. Spyrou[1,2], Aida Andrades Valtueña[1], Daniel Huson[5], Noreen Tuross[2]*, Kirsten I. Bos[1,2]* and Johannes Krause[1,2]*

Affiliations:

[1]Max Planck Institute for the Science of Human History, Jena, Germany.

[2]Institute for Archaeological Sciences, University of Tübingen, Tübingen, Germany

[3]Department of Human Evolutionary Biology, Harvard University, Cambridge, MA, USA.

[4]Institute of Evolutionary Medicine, University of Zurich, Zurich, Switzerland.

[5]INAH, National Institute of Anthropology and History, Mexico, Teposcolula-Yucundaa Archaeological Project.

[6]Center for Bioinformatics Tübingen (ZBIT), University of Tübingen, Tübingen, Germany.

[#]These authors contributed equally to this work

*Correspondence to: A.H.: herbig@shh.mpg.de; N.T.: tuross@fas.harvard.edu; K.I.B.: bos@shh.mpg.de; J.K.: krause@shh.mpg.de

†Current address: M.G.C.: Smithsonian Conservation Biology Institute, Center for Conservation Genomics, 3001 Connecticut Avenue NW, Washington, DC 20008, USA.

Summary paragraph: Indigenous populations of the Americas experienced high mortality rates during the early contact period as a result of infectious diseases, many of which were introduced by Europeans. Most of the pathogenic agents that caused these outbreaks remain unknown. Through the introduction of a new metagenomic analysis tool called MALT applied here to search for traces of ancient pathogen DNA, we were able to identify *Salmonella enterica* in individuals buried in an early contact era epidemic cemetery at Teposcolula-Yucundaa, Oaxaca in southern Mexico. This cemetery is linked, based on historical and archaeological evidence, to the 1545-1550 CE epidemic that affected large parts of Mexico. Locally this epidemic was known as "*cocoliztli*", the pathogenic cause of which has been debated for over a century. Here we present genome-wide data from ten individuals for *Salmonella enterica* subsp. *enterica* serovar Paratyphi C, a bacterial cause of enteric fever. We propose that *S.* Paratyphi C be considered a strong candidate for the epidemic population decline during the 1545 *cocoliztli* outbreak at Teposcolula-Yucundaa.

Infectious diseases introduced to the New World following European contact led to successive outbreaks in many regions of the Americas that continued well into the 19th century. These often caused high mortality and thus contributed a central, and often underappreciated, influence on the demographic collapse of many indigenous populations[1-4]. Population declines linked to regionally specific epidemics are estimated to have reached as high as 95%[3], and their genetic impact based on recent population-based studies of ancient and modern human exome and mitochondrial data attest to their scale[5,6]. One hypothesis posits that the increased susceptibility of New World populations to Old World diseases facilitated European conquest, whereby rapidly disseminating diseases severely weakened indigenous populations[2], in some cases even in advance of European presence in the region[2,7]. Well-characterized infections such as smallpox, measles, mumps, and influenza are known causes of later contact era outbreaks; however, the diseases responsible for many early contact period New World epidemics remain unknown and have been the subject of scientific debate for over a century[2-4,7,8].

Morphological changes in skeletal remains[9] and ethnohistorical accounts[10] are often explored as sources for understanding population health in the past, although both provide only limited resolution and have generated speculative and at times conflicting hypotheses about the diseases introduced to New World populations[2,3,7,11,12]. Most infectious diseases do not leave characteristic markers on the skeleton due to either their short periods of infectivity, the death of the victim in the acute phase before skeletal changes formed, or a lack of osteological involvement[9]. While historical descriptions of infectious disease symptoms can be detailed, they are subject to cultural biases, suffer from translational inaccuracies, lack a foundation in germ theory, and describe historical forms of a condition that may differ from modern manifestations[8,11]. Additionally, differential diagnosis based on symptoms alone can be

unreliable even in modern contexts since many infectious diseases have similar clinical presentations.

Genome-wide studies of ancient pathogens have proven instrumental in both identifying and characterizing past human infectious diseases. These studies have largely been restricted to skeletal collections where individuals display physical changes consistent with particular infections[13-15], an historical context that links a specific pathogen to a known epidemiological event[16], or an organism that was identified via targeted molecular screening without prior indication of its presence[17]. Recent attempts to circumvent these limitations have concentrated on broad-spectrum molecular approaches focused on pathogen detection via fluorescence-hybridization-based microarray technology[18], identification via DNA-enrichment of certain microbial regions[19] or computational screening of non-enriched sequence data against human microbiome data sets[20]. These approaches offer improvements, but remain biased in the bacterial taxa used for species-level assignments. As archaeological material is expected to harbour an abundance of bacteria that stem from the depositional context, omission of environmental taxa in species assignments can lead to false-positive identifications. Additional techniques for authenticating ancient DNA have been developed[21,22], including the identification of characteristic damage patterns caused by the deamination of cytosines[23], methods that evaluate evenness of coverage of aligned reads across a reference genome, or length distributions that consider the degree of fragmentation, where ancient molecules are expected to be shorter than those from modern contaminants[24].

A typical NGS dataset from an ancient sample comprises millions of DNA sequencing reads, making taxonomic assignment and screening based on sequence alignments computationally challenging. The gold standard tool for alignment-based analyses is BLAST[25], due to its

sensitivity and statistical model. However, the computational time and power BLAST requires to analyse a typical metagenomic dataset is often prohibitive.

Here we introduce MALT (**M**EGAN **AL**ignment **T**ool), a program for the fast alignment and analysis of metagenomic DNA sequencing data. MALT contains the same taxonomic binning algorithm, i.e. the naïve LCA (Lowest Common Ancestor) algorithm (for reviews see[26,27]), implemented in the interactive metagenomics analysis software MEGAN[28]. Like BLAST, MALT computes "local" alignments between highly conserved segments of reads and references. MALT can also calculate "semi-global" alignments where reads are aligned end-to-end. In comparison to protein alignments or local DNA alignments, semi-global DNA alignments are more suitable for assessing various quality and authenticity criteria that are commonly applied in the field of paleogenetics.

We applied our MALT screening pipeline (Supplementary Figures 1, 2) using a database of all complete bacterial genomes available in NCBI RefSeq to non-enriched DNA sequence data from the pulp chamber of teeth collected from indigenous individuals excavated at the site of Teposcolula-Yucundaa, located in the highland Mixteca Alta region of Oaxaca, Mexico[29,30]. The site contains both pre-contact and contact era burials, including the earliest identified contact era epidemic burial ground in Mexico[30,31] (Fig. 1; Supplementary methods 1). This is the only known cemetery historically linked to the *cocoliztli* epidemic of 1545-1550 CE[30], described as one of the principal epidemiological events responsible for the cataclysmic population decline of 16th century Mesoamerica[7,32]. This outbreak affected large areas of central Mexico and Guatemala, spreading perhaps as far south as Peru[7,30]. Via the MALT screening approach, we were able to identify ancient *Salmonella enterica* DNA in the sequence data generated from this archaeological material, to the exclusion of DNA

stemming from the complex environmental background. While the pathogenic cause of the *cocoliztli* epidemic is ambiguous based on ethnohistorical evidence[7,8,30], we report the first molecular evidence of microbial infection with genome-wide data from *S. enterica* subsp. *enterica* serovar Paratyphi C (enteric fever) isolated from ten epidemic-associated contact era burials.

Results

The individuals included in this investigation were excavated from the contact era epidemic cemetery located in the Grand Plaza (administrative square) (n=24) and the pre-contact churchyard cemetery (n=5) at Teposcolula-Yucundaa between 2004 and 2010[30] (Fig. 1; Supplementary Table 1; Supplementary methods 1). Previous work demonstrated ancient DNA preservation at the site through the identification of New World mitochondrial haplogroups in 48 individuals, 28 of which overlap with this study[30]. Additionally, oxygen isotope analysis identified them as local inhabitants[30]. Thirteen individuals included in this study were previously radiocarbon dated[31] yielding dates that support archaeological evidence that the Grand Plaza (n=10) and churchyard (n=3) contain contact and pre-contact era burials, respectively (Supplementary Table 1). The Grand Plaza is estimated to contain more than 800 individuals, mostly interred in graves containing multiple persons. Those excavated contribute to a demographic profile consistent with an epidemic event[29,30].

Tooth samples were processed according to protocols designed for ancient DNA work (Supplementary methods 2). An aggregate soil sample from the two burial grounds was analysed in parallel to gain an overview of environmental bacteria that may have infiltrated our samples. Pre-processed sequencing data of approximately one million paired-end reads per tooth were analysed with MALT using a curated reference database of 6247 complete

bacterial genomes, comprising all those available in NCBI RefSeq (December 2016). Our approach limits ascertainment biases and false positive assignments that could result from databases deficient in environmental taxa (Supplementary methods 3). A runtime analysis revealed a 200-fold improvement in computation time for MALT in comparison to BLASTn (see Methods). Results were visualized in MEGAN[28] and taxonomic assignments were evaluated with attention to known pathogenic species. Reads taxonomically assigned by MALT ranged from 4,842 to 44,315 for the samples. Assigned reads belonging to bacterial constituents of human oral and soil microbiota are present in varying proportions amongst the samples (Fig. 2; Supplementary Table 2). Of note, three teeth (Tepos_10, Tepos_14 and Tepos_35) had between 365 to 659 reads assigned to *Salmonella enterica*, a known cause of enteric fever in humans today. Of the *S. enterica* strains present in the database, *S.* Paratyphi C had the highest number of assigned reads (Supplementary methods 3; Supplementary Table 2). Mapping these three metagenomic datasets to the *S.* Paratyphi C RKS4594 genome (NC_012125.1) revealed the characteristic pattern of damage expected of ancient DNA (Supplementary Fig. 3; Supplementary methods 3; Supplementary Table 4). Subsequently, the sequencing data for all samples was mapped to the human genome (hg19), revealing a similar level of damage in the human reads for Tepos_10, Tepos_14 and Tepos_35, thus providing further support for the ancient origin of the *S. enterica* reads (Supplementary methods 4; Supplementary Table 5). An additional seven individuals from the Grand Plaza cemetery and one negative control harboured low numbers of assigned *S. enterica* reads ranging from 4 to 51 (Supplementary Table 2). These were considered as potential weak-positive samples. One negative control was found to contain 15 reads assigned to *S. enterica*, and a further four contained one or two reads, as did nine sample libraries, seven of which were not included in downstream analyses. The soil library and remaining sample libraries were void of *S. enterica* reads (Fig. 2; Supplementary methods 3; Supplementary Table 2).

An additional MALT screen for traces of viral DNA revealed one notable taxonomic hit to *Salmonella* phage Vi II-E1, a phage associated with *Salmonella* serovars that produce the Vi capsule antigen[33], which includes *S*. Paratyphi C (Supplementary methods 3; Supplementary Table 3).

To further authenticate and elucidate our findings we performed whole-genome targeted array and in-solution hybridization capture[34,35], using probes designed to encompass modern *S. enterica* genome diversity (Supplementary methods 5, 6, 7; Supplementary Table 6). All five pre-contact samples, the soil sample, one post-contact sample putatively negative for *S. enterica* based on our MALT screening, all negative controls, and both UDG-treated (DNA damage removed) and non-UDG treated libraries from the ten putatively positive samples (Tepos_10, Tepos_11, Tepos_20, Tepos_14, Tepos_34, Tepos_35, Tepos_36, Tepos_37, Tepos_38, Tepos_41) were included in the capture (Supplementary methods 6, 7).

Mapping and genotyping of the captured Illumina sequenced reads was performed using the *S.* Paratyphi C reference genome (NC_012125.1) (Supplementary methods 6, 7, 8; Supplementary Table 7). Capture of *S. enterica* DNA was successful for the ten positive samples yielding a minimum of 33,327 unique reads per UDG treated library. The remaining bone samples, soil sample, and negative controls were determined to be negative for ancient *S. enterica* DNA with the exception of one negative control (EB2-091013) that had likely become cross-contaminated during processing (see Supplementary methods 8; Supplementary Table 7). Five complete genomes were constructed for Tepos_10, Tepos_14, Tepos_20, Tepos_35 and Tepos_37, covering 95%, 97%, 67%, 98% and 74% of the reference at a minimum of 3-fold coverage and yielding an average genomic coverage of 33-, 36-, 4.6-, 96- and 5.5-fold, respectively (Table 1). Artificial reads generated *in silico* for 23

complete genomes included in the probe design were also mapped to the *S.* Paratyphi C RKS4594 reference (Supplementary methods 8; Supplementary Table 6) and phylogenetic comparison revealed that the five ancient genomes clustered with *S.* Paratyphi C (Fig. 3; Supplementary Figures 4, 6; Supplementary methods 8). The phylogenetic positioning was retained when the whole dataset was mapped to and genotyped against the *S.* Typhi CT18 reference genome (NC_003198.1) (Supplementary Figure 5; Supplementary Table 8), the most common bacterial cause of enteric fever in humans today. This result excludes the possibility of a reference bias. Despite all five ancient genomes being contemporaneous, the Tepos_10 genome was observed to contain many more derived positions. An investigation of heterozygous variant calls showed that Tepos_10 has a much higher number of heterozygous sites. We believe this is best explained by the presence of genetically similar non-target DNA that co-enriched in the capture for this sample alone. Based on the pattern of allele frequencies, this genome was excluded from downstream analyses (Supplementary methods 9; Supplementary Figure 7). Tepos_20 and Tepos_37 were also excluded due to their genomic coverage of less than 6-fold, which allowed more reliable SNP calling at a minimum of 5-fold coverage for Tepos_14 and Tepos_35. Subsequent phylogenetic tree construction with 1000 bootstrap replicates revealed 100% support and branch shortening for the Tepos_14 and Tepos_35 genomes in all phylogenies, supporting their ancient origin (Fig. 3; Supplementary Figure 8).

SNP analysis for the ancient genomes together with the reference dataset yielded a total of 203,256 variant positions amongst all 25 genomes. Our analyses identified 681 positions present in one or both of the ancient genomes, where 133 are unique to the ancient lineage (Supplementary methods 10; Supplementary Table 9). Of these, 130 unique SNPs are shared between Tepos_14 and Tepos_35, supporting their close relationship and shared ancestry.

The *ydiD* gene involved in the breakdown of fatty acids[36] and the *tsr* gene related to the chemotaxic response system[37] were found to contain multiple non-synonymous SNPs (nsSNPs) unique to the ancient genomes (Supplementary methods 10). Seven homoplastic and four tri-allelic variant positions were detected in the ancient genomes (Supplementary methods 10; Supplementary Tables 10a, 10b).

A region of the *pil* operon consisting of five genes, *pilS*, *pilU*, *pilT*, *pilV* and *rci,* was found in our ancient genomes and was absent in the *S.* Paratyphi C RKS4594 genome[38] (Supplementary methods 12; Supplementary Table 12). This region is located in Salmonella Pathogenicity Island 7 (SPI-7), and encodes a type IVB pili[39,40]. The version of *pilV* in our ancient genomes is thought to facilitate bacterial self-aggregation, a phenomenon that potentially aids in invasion of host tissues[39,40] (for details see Supplementary methods 12). A presence/absence analysis of virulence factors was also conducted (Supplementary methods 13; Supplementary Table 13; Supplementary Figure 9).

The *S.* Paratyphi C RKS4594 strain harbours a virulence plasmid, pSPCV, which was included in our capture design. It is present at 10- to 224-fold average coverage for the five genomes (Supplementary methods 14; Supplementary Tables 14, 15).

Non-UDG capture reads mapped to the *S*. Paratyphi C genome (NC_012125.1) for Tepos_11, Tepos_34, Tepos_36, Tepos_38 and Tepos_41, i.e. those that did not yield full genomes, had damage patterns characteristic of ancient DNA (Supplementary Figure 3). To further verify these reads as true ancient *S*. Paratyphi C reads we investigated 45 SNPs unique to Tepos_14 and Tepos_35 that are included in our phylogenetic analysis (Supplementary methods 11; Supplementary Table 11). Of the 45 positions, between 6 and 29 had a minimum of 1-fold

coverage in these low coverage libraries. All of these were in agreement with the unique SNPs present in the high-coverage ancient genomes, thus confirming their shared ancestry.

Discussion

Interpretations of ethnohistorical documents have suggested some form of typhus or enteric (typhoid/paratyphoid) fever (from the Spanish "tabardillo", "tabardete", and "*tifus mortal"*), viral haemorrhagic fever, measles, or pneumonic plague as potential causes of the *cocoliztli* epidemic of 1545 CE (for ref. see Supplementary discussion 1). These diseases present symptoms similar to those that were recorded in the *cocoliztli* outbreak such as red spots on the skin, bleeding from various body orifices, and vomiting (Supplementary discussion 1; Supplementary Figure 10). Given the non-specific nature of these symptoms, additional sources of data are needed to clarify which disease(s) was/were circulating. Previous investigation of sequencing data generated from the Teposcolula-Yucundaa material did not identify DNA traces of ancient pathogens; however, *S. enterica* was not considered as a candidate[41]. Here we have isolated genome-wide data of ancient *S.* Paratyphi C from ten Mixtec individuals buried in the *Grand Plaza* epidemic cemetery at Teposcolula-Yucundaa, indicating that enteric fever was circulating in the indigenous population during the *cocoliztli* epidemic of 1545-50 CE. As demonstrated here, MALT offers a sensitive approach for screening non-enriched sequence data in search for unknown candidate bacterial pathogens involved in past disease outbreaks, even to the exclusion of a dominant environmental microbial background. Most importantly, it offers the advantage of extensive genome-level screening without the need to specify a target organism, thus avoiding ascertainment biases common to other screening approaches. Fast metagenomic profiling tools that are based on k-mer matching such as KRAKEN[42] or specific diagnostic marker regions such as MetaPhlan2[43] have limitations in ancient DNA applications. Complete alignments are needed

to authenticate candidate taxonomic assignments, and a small number of marker regions might not provide sufficient resolution for identification, as target DNA is often present in low amounts. Our focus on only bacterial and DNA viral taxa limits our resolution in identifying other infectious agents that may have been present in the population during the Teposcolula-Yucundaa epidemic.

Although our discussions here have focused on a single pathogenic organism, the potential of its having acted synergistically with other pathogen(s) circulating during the epidemic must be considered. The concept of syndemics and the complex biosocial factors that influence infectious disease transmission and severity are well-documented in both modern and historical contexts[44,45]. We are currently limited to the detection of bacterial pathogens and DNA viruses included in the NCBI genomic database, though the resolution offered by MALT analyses will increase as this database grows. We have not investigated the presence of RNA viruses, since methods for RNA retrieval from archaeological tissues are underdeveloped and not supported by our current protocols[46].

We confidently exclude an environmental organism as the source for our ancient genomes on the basis that 1) *S.* Paratyphi C is restricted to humans, 2) it is not known to freely inhabit soil (our soil sample was negative for *Salmonella* during screening and after capture), 3) the deamination patterns observed for the ancient human and *S.* Paratyphi C reads are characteristic of authentic ancient DNA, and 4) the ancient *S.* Paratyphi C genomes display expected branch-shortening in all constructed phylogenies. Moreover, we recovered all ancient genomic data from the pulp-chambers of teeth collected *in situ*, increasing the likelihood of our having identified a bacterium that was present in the victim's blood at the time of death. *S. enterica* introduction via post-burial disturbance is unlikely because the

graves in the *Grand Plaza* were dug directly into the thickly paved floor at the site and historical records indicate that Teposcolula-Yucundaa was abandoned shortly after the epidemic ended in 1552 CE[29,30].

S. Paratyphi C is one of over 2600 identified *S. enterica* serovars distinguished by their antigenic formula[47]. Only four serovars (*S.* Typhi and *S.* Paratyphi A, B, C), all of which cause enteric fever, are restricted to the human host[47]. Today *S.* Typhi and *S.* Paratyphi A cause the majority of reported cases[48]. *S.* Paratyphi C is rarely reported[38,48]. Infected individuals shed bacteria long after the termination of symptoms[47], and in the case of *S.* Typhi infection, 1-6% of individuals become asymptomatic carriers[49]. Following the hypothesis that this disease was introduced via European contact, it is conceivable that asymptomatic European carriers who withstood the cross-Atlantic voyage could have introduced *S.* Paratyphi C to Mesoamerican populations in the 16th century. First hand descriptions of the 1545 *cocoliztli* epidemic suggest that both European and Mixtec individuals were susceptible to the disease[7,50], with one estimate of a 60-90% population decline in New Spain during this period[7].

The additional SPI-7 genes detected through indel analysis are reported to vary in presence/absence amongst modern *S.* Paratyphi C strains[38,40], and are suspected to cause increased virulence when the inverted repeats in *pilV* allow the Rci recombinase to shuffle between its two protein states (Supplementary methods 12). This may support an increased capacity for our ancient strains to cause an epidemic outbreak. However, the overall mechanisms through which *S.* Paratyphi causes enteric fever remain unclear. The nsSNPs in the *ydiD* and *tsr* genes may signify adaptive processes, and comparison with a greater number of *S.* Paratyphi C genomes may clarify this[51].

311

312 Today, *S*. Paratyphi C is rare in Europe and the Americas, with more cases identified across
313 Africa and Asia[52,53]. Based on MLST data from modern *S.* Paratyphi C strains, no clear
314 phylogeographic pattern has been observed[52]. However, the presence of a 1200 CE *S.*
315 Paratyphi C genome in Norway indicates its presence in Europe in the pre-contact era[51],
316 which would be necessary for it to be considered an Old World disease. However, based on
317 the small number of pre-contact individuals that we have screened, we cannot exclude the
318 presence of *S.* Paratyphi C at Teposcolula-Yucundaa prior to European arrival. A local origin
319 for the *cocoliztli* disease has been proposed elsewhere[54]. Historical accounts offer little
320 perspective on its origin since neither the indigenous population nor the European colonizers
321 had a pre-existing name for the disease[7,8,30]. Spanish colonial documents refer to it as
322 *pujamiento de sangre* ('full bloodiness'), while the indigenous Aztec population of Central
323 Mexico called it *cocoliztli*, a generic term meaning 'pestilence' in Nahuatl[7,8] (see
324 Supplementary discussion 1).

325

326 Little is known about the past severity and worldwide incidence of enteric fever, first
327 determined to be distinct from typhus in the mid-nineteenth century[55]. Enteric fevers are
328 regarded as major health threats across the world[48], causing an estimated ~27 million
329 illnesses in 2000, the majority of which were attributed to *S*. Typhi[56]. Due to the rarity of *S.*
330 Paratyphi C diagnoses, mortality rates are not established for this particular serovar. Today,
331 outbreaks predominantly occur in developing countries. *S.* Typhi/Paratyphi are commonly
332 transmitted through the faecal-oral route via ingestion of contaminated food or water[57].
333 Changes imposed under Spanish rule such as forced relocations under the policy of
334 *congregación*, altered living arrangements, and new subsistence farming practices[29,30]

compounded by drought conditions[32] could have disrupted existing hygiene measures, facilitating *S.* Paratyphi C transmission.

Our study represents a first step towards a molecular understanding of disease exchange in contact era Mexico. The 1545 *cocoliztli* epidemic is regarded as one of the most devastating epidemics in New World history[7,32]. Our findings contribute to the debate concerning the causative agent of this epidemic at Teposcolula-Yucundaa, where we propose that *S.* Paratyphi C be considered. We introduced MALT, a novel fast alignment and taxonomic assignment method. Its application to the identification of ancient *Salmonella enterica* DNA within a complex background of environmental microbial contaminants speaks to the suitability of this approach, and its resolution will improve as the number of available reference genomes increases. This method may be eminently useful for studies wishing to identify pathogenic agents involved in ancient and modern disease, particularly in cases where candidate organisms are not known *a priori.*

Methods

The MALT algorithm

MALT is based on the seed-and-extend paradigm and consists of two programs, *malt-build* and *malt-run*.

First, *malt-build* is used to construct an index for the given database of reference sequences. To do so, malt-build determines all occurrences of spaced seeds[58-60] in the reference sequences and places them into a hash table[61].

Following this, *malt-run* is used to align a set of query sequences against the reference database. To this end, the program generates a list of spaced seeds for each query and then looks them up in the reference hash table, which is kept in main memory. Using the x-drop extension heuristic[25], a high-scoring ungapped alignment anchored at the seed is computed and is used to decide whether or not a full alignment should be constructed. Local or semi-global alignments are computed using a banded implementation[62] of the Smith-Waterman[63] or Needleman-Wunsch[64] algorithms, respectively. The program then computes the bit-score and expected value (E-value) of the alignment and decides whether to keep or discard the alignment depending on user-specified thresholds for bit-score, E-value or percent identity. The application of *malt-run* is illustrated in Supplementary Figure 1.

The MALT screening pipeline

In order to use MALT in ancient DNA contexts to screen for bacterial DNA and to assess the taxonomic composition of ancient bacterial communities we applied the following workflow (Supplementary Figure 2). First we used *malt-build* to construct a MALT index on all complete bacterial genomes in GenBank[65]. This was done only once, and is rebuilt only when the target database requires updating. We align reads to the reference database using *malt-run*

390 in semi-global mode. MALT generates output in RMA format and in SAM format. The
391 former can be used for interactive analysis of taxonomic composition in MEGAN[28] and the
392 latter for alignment-based assessment of damage patterns and other authenticity criteria.
393
394 **Sample provenience**
395 The site of Teposcolula-Yucundaa is situated on a mountain ridge in the Mixteca Alta region
396 of Oaxaca, Mexico. Prior archaeological excavation at this site revealed a large epidemic
397 cemetery located in the Grand Plaza – the town's administrative centre, and an additional
398 cemetery in the churchyard (Fig. 1; Supplementary methods 1). 24 teeth were collected from
399 individuals buried in the Grand Plaza cemetery and 5 were collected from the individuals
400 buried in the churchyard cemetery (Supplementary methods 2; Supplementary Table 1). Soil
401 samples were also collected from both cemetery sites (Supplementary methods 2).
402
403 **DNA extraction and library preparation**
404 DNA extracts and double-stranded indexed libraries compatible with Illumina sequencing
405 were generated using methods tailor-made for ancient DNA[66-68]. This work was carried out in
406 dedicated ancient DNA cleanroom facilities at the University of Tübingen and Harvard
407 University (Supplementary methods 2).
408
409 **Screening with MALT**
410 Amplified libraries were shotgun sequenced. The reads were adapter clipped and merged
411 before being analysed with MALT and the results visualized in MEGAN6[28] (Supplementary
412 methods 2, 3). Two MALT runs were executed. The first using all complete bacterial
413 genomes available through NCBI RefSeq (December, 2016), and the second using the full
414 NCBI Nucleotide (nt) database (ftp://ftp-trace.ncbi.nih.gov/blast/db/FASTA/) as reference to

screen for viral DNA (Fig. 2; Supplementary methods 3; Supplementary Tables 2, 3). Both runs used 'semi-global' alignment and a minimum percent identity of 95% (Supplementary methods 3). The shotgun data was also mapped to the *S.* Paratyphi C RKS4594 reference (NC_012125.1) and the human genome (hg19) and damage plots were generated (Supplementary methods 3, 4; Supplementary Table 4, 5; Supplementary Figure 3).

Runtime comparison

The programs MALT (version 0.3.8) and BLAST[25] (version 2.6.0+) were applied to the shotgun screening data of Tepos_35 consisting of altogether 952,511 reads. For both programs the DNA alignment mode (blastn) was chosen. The maximal E-value was set to 1.0. The maximal number of alignments for each query was set to 100. The minimal per cent identity was set to 95. The number of threads was set to 16. The alignment type of MALT was set to 'Local' in order to be comparable to BLAST. The total amount of RAM required by MALT during this run was 252.7 GB.

For MALT the runtime was measured excluding the initial loading of our reference database, which happens only once when screening multiple samples. The loading of the database takes 27.27 minutes. Including taxonomic binning the application of MALT to our complete shotgun screening data took 123.36 minutes. As a comparison, processing only the screening data of a single sample (Tepos_35) with BLASTn took 1420.58 minutes without any taxonomic analysis. Processing of this sample alone with MALT, including taxonomic binning, took 6.48 minutes, which constitutes a 200-fold improvement in terms of computation time.

The computations were performed on a Dell PowerEdge R820 with four Intel Xeon E5-4620 2.2 GHz CPUs und 768 GB RAM.

Probe design and whole-genome capture

Array probes were designed based on 67 publicly available *S. enterica* chromosomes/assemblies and 45 associated plasmid sequences (Supplementary methods 5; Supplementary Table 6). Extracts from samples deemed to be positive for *S. enterica* Paratyphi C were converted into additional rich UDG-treated libraries[69] for whole-genome capture (Supplementary methods 6, 7). Pre-contact and post-contact samples were serially captured using our custom probe design, according to two established methods[35,70]. The eluate from both array and in-solution capture was sequenced to a sufficient depth to allow high coverage genome reconstruction (Supplementary methods 6, 7).

Sequence data processing, initial phylogenetic assessment and authenticity

The sequence data was adapter clipped and quality filtered before being mapped to the *S.* Paratyphi C reference (NC_012125.1) (Supplementary methods 8; Supplementary Table 7). Deamination patterns for the DNA were generated to assess the authenticity of the ancient *S.* Paratyphi C DNA using mapDamage[23] (Supplementary methods 8; Supplementary Table 7; Supplementary Figure 3). Artificial read data was generated for a dataset of 23 genomes selected for comparative phylogenetic analysis; this data was also mapped to the *S.* Paratyphi C reference (Supplementary methods 8). SNP calling was carried out with GATK using a quality score of ≥30 for the five *S.* Paratyphi C genomes and the artificial read dataset. A neighbor-joining tree was constructed using MEGA6[71], based on a homozygous SNPs called at a minimum of 3-fold coverage where at least 90% of reads are in agreement (Supplementary methods 8; Supplementary Figure 4). In order to exclude a reference bias in the ascertainment of the phylogenetic positioning of the five ancient genomes (Tepos_10, Tepos_14 Tepos_20, Tepos_35 and Tepos_37), mapping, SNP calling and tree construction

464 was repeated for the *S.* Typhi CT18 reference (NC_003198.1) (Supplementary methods 8;
465 Supplementary Table 8; Supplementary Figure 5).
466
467 **SNP typing and phylogenetic analysis**
468 Homozygous SNPs were called from the complete dataset (5 ancient and 23 modern) based
469 on our criteria using a tool called MultiVCFAnalyzer (Supplementary methods 9). Repetitive
470 and highly conserved regions of the *S.* Paratyphi C genome (NC_012125.1) were excluded
471 from SNP calling to avoid spurious mapping reads. Maximum Parsimony[71] and a Maximum
472 Likelihood[72] trees were made including the five genomes (Fig. 3; Supplementary Figure 6).
473 Heterozygous positions were also called and their allele frequency distributions plotted using
474 R[73] (Supplementary methods 9; Supplementary Figure 7). SNP calling and phylogenetic tree
475 construction was repeated excluding the Tepos_10, Tepos_20 and Tepos_37 genomes
476 (Supplementary methods 10; Fig. 3; Supplementary Figure 8).
477
478 The five weak-positive samples: Tepos_11, Tepos_34, Tepos_36, Tepos_38 and Tepos_41,
479 that did not yield enough data for genome reconstruction, were investigated for 46 SNPs
480 unique to the ancient genomes to verify that the captured reads for these samples are true
481 ancient *S*. Paratyphi C reads (Supplementary methods 11; Supplementary Table 11).
482
483 **SNP effect and Indel analyses**
484 SNP effect analysis was carried out for the two ancient genomes (Tepos_14 and Tepos_35)
485 alongside the modern dataset (see Supplementary methods 10). SNPs unique to the ancient
486 genomes, pseudogenes and homoplastic positions were investigated (Supplementary methods
487 10; Supplementary Tables 9, 10). Insertions and deletions (Indels), 700bp or larger, in the
488 two ancient genomes were identified through two approaches. Deletions were visually

detected by mapping the ancient data to the *S*. Paratyphi C reference using a mapping quality threshold (-q) of 0 and manually viewing the genome alignment in the IGV browser (Supplementary methods 12). In order to detect insertions, or regions present in the ancient genomes that are missing the modern reference, the ancient data was mapped to concatenated reference pairs. Where one reference was in all cases the *S.* Paratyphi C RKS4594 reference (NC_012125.1) and the other was one of four *S. enterica* genomes of interest. A mapping quality threshold (-q) of 37 was used, thus allowing only regions unique to one or the other genome in the pair to map (Supplementary methods 12; Supplementary Table 12).

Virulence factor analysis

43 effector genes identified within *Salmonella enterica subsp. enterica*[74] were investigated using the BEDTools suite[75]. The percentage of each gene that was covered at least 1-fold in the ancient and modern genomes in our dataset was plotted using the ggplot2package[76] in R[73] (Supplementary methods 13; Supplementary Figure 9).

Plasmid analysis

The ancient data was mapped to the *S*. Paratyphi C virulence plasmid, pSPCV. SNP effect analysis was carried out in comparison to three other similar plasmid references (Supplementary methods 14; Supplementary Tables 14, 15).

Data Availability

Sequence data that support the findings of this study have been submitted to the European Nucleotide Archive under accession number PRJEB23438. MALT is open source and freely available from: http://ab.inf.uni-tuebingen.de/software/malt. The program MultiVCFAnalyzer is available on GitHub: https://github.com/alexherbig/MultiVCFAnalyzer. Source data for

figures are available upon request.

References:

1 Ubelaker, D. H. Prehistoric New World population size: Historical review and current appraisal of North American estimates. *Am J Phys Anthropol* **45**, 661-665, doi:10.1002/ajpa.1330450332 (1976).

2 Crosby, A. W. Virgin soil epidemics as a factor in the aboriginal depopulation in America. *William Mary Q* **33**, 289-299 (1976).

3 Dobyns, H. F. Disease Transfer at Contact. *Annu Rev Anthropol* **22**, 273-291 (1993).

4 Acuna-Soto, R., Stahle, D. W., Therrell, M. D., Griffin, R. D. & Cleaveland, M. K. When half of the population died: the epidemic of hemorrhagic fevers of 1576 in Mexico. *FEMS Microbiol Lett* **240**, 1-5, doi:10.1016/j.femsle.2004.09.011 (2004).

5 Llamas, B. *et al.* Ancient mitochondrial DNA provides high-resolution time scale of the peopling of the Americas. *Sci Adv* **2**, e1501385, doi:10.1126/sciadv.1501385 (2016).

6 Lindo, J. *et al.* A time transect of exomes from a Native American population before and after European contact. *Nat Commun* **7**, 13175, doi:10.1038/ncomms13175 (2016).

7 Cook, N. D. & Lovell, W. G. *Secret Judgments of God: Old World Disease in Colonial Spanish America*. (University of Oklahoma Press, 2001).

8 Fields, S. L. *Pestilence and Headcolds: Encountering Illness in Colonial Mexico*. (Columbia University Press, 2008).

9 Ortner, D. J. *Identification of pathological conditions in human skeletal remains*. 2 edn, (Academic Press, 2003).

10 Walker, R. S., Sattenspiel, L. & Hill, K. R. Mortality from contact-related epidemics among indigenous populations in Greater Amazonia. *Sci Rep* **5**, 14032, doi:10.1038/srep14032 (2015).

11 Joralemon, D. New World Depopulation and the Case of Disease. *J Anthropol Res* **38**, 108-127 (1982).

12 Larsen, C. S. In the wake of Columbus: Native population biology in the postcontact Americas. *Am J Phys Anthropol* **37**, 109-154, doi:10.1002/ajpa.1330370606 (1994).

13 Bos, K. I. *et al.* Pre-Columbian mycobacterial genomes reveal seals as a source of New World human tuberculosis. *Nature* **514**, 494-497, doi:10.1038/nature13591 (2014).

14 Schuenemann, V. J. *et al.* Genome-wide comparison of medieval and modern Mycobacterium leprae. *Science* **341**, 179-183, doi:10.1126/science.1238286 (2013).

15 Warinner, C. *et al.* Pathogens and host immunity in the ancient human oral cavity. *Nat Genet* **46**, 336-344, doi:10.1038/ng.2906 (2014).

16 Bos, K. I. *et al.* A draft genome of Yersinia pestis from victims of the Black Death. *Nature* **478**, 506-510, doi:10.1038/nature10549 (2011).

17 Maixner, F. *et al.* The 5300-year-old Helicobacter pylori genome of the Iceman. *Science* **351**, 162-165, doi:10.1126/science.aad2545 (2016).

18 Devault, A. M. *et al.* Ancient pathogen DNA in archaeological samples detected with a Microbial Detection Array. *Sci Rep* **4**, 4245, doi:10.1038/srep04245 (2014).

19 Bos, K. I. *et al.* Parallel detection of ancient pathogens via array-based DNA capture. *Philosophical transactions of the Royal Society of London. Series B, Biological sciences* **370**, 20130375, doi:10.1098/rstb.2013.0375 (2015).

20 Devault, A. M. *et al.* A molecular portrait of maternal sepsis from Byzantine Troy. *Elife* **6**, doi:10.7554/eLife.20983 (2017).

21 Warinner, C. *et al.* A Robust Framework for Microbial Archaeology. *Annu Rev Genomics Hum Genet*, doi:10.1146/annurev-genom-091416-035526 (2017).

22 Key, F. M., Posth, C., Krause, J., Herbig, A. & Bos, K. I. Mining Metagenomic Data Sets for Ancient DNA: Recommended Protocols for Authentication. *Trends Genet* **33**, 508-520, doi:10.1016/j.tig.2017.05.005 (2017).

23 Jonsson, H., Ginolhac, A., Schubert, M., Johnson, P. L. & Orlando, L. mapDamage2.0: fast approximate Bayesian estimates of ancient DNA damage parameters. *Bioinformatics* **29**, 1682-1684, doi:10.1093/bioinformatics/btt193 (2013).

24 Prufer, K. *et al.* Computational challenges in the analysis of ancient DNA. *Genome Biol* **11**, R47, doi:10.1186/gb-2010-11-5-r47 (2010).

25 Altschul, S. F., Gish, W., Miller, W., Myers, E. W. & Lipman, D. J. Basic local alignment search tool. *J Mol Biol* **215**, 403-410, doi:10.1016/S0022-2836(05)80360-2 (1990).

26 Peabody, M. A., Van Rossum, T., Lo, R. & Brinkman, F. S. Evaluation of shotgun metagenomics sequence classification methods using in silico and in vitro simulated communities. *BMC Bioinformatics* **16**, 363, doi:10.1186/s12859-015-0788-5 (2015).

27 Lindgreen, S., Adair, K. L. & Gardner, P. P. An evaluation of the accuracy and speed of metagenome analysis tools. *Sci Rep* **6**, 19233, doi:10.1038/srep19233 (2016).

28 Huson, D. H. *et al.* MEGAN Community Edition - Interactive Exploration and Analysis of Large-Scale Microbiome Sequencing Data. *PLoS Comput Biol* **12**, e1004957, doi:10.1371/journal.pcbi.1004957 (2016).

29 Spores, R. & Robles García, N. A prehispanic (postclassic) capital center in colonial transition: excavations at Yucundaa Pueblo Viejo de Teposcolula, Oaxaca, Mexico. *Lat Am Antiq* **18**, 33-353 (2007).

30 Warinner, C., Robles García, N., Spores, R. & Tuross, N. Disease, Demography, and Diet in Early Colonial New Spain: Investigation of a Sixteenth-Century Mixtec Cemetery at Teposcolula Yucundaa. *Lat Am Antiq* **23**, 467-489 (2012).

31 Tuross, N., Warinner, C. & Robles García, N. in *Yucundaa: La cuidad mixteca Yucundaa-Pueblo Viejo de Teposcolula y su transformación prehispánica-colonial* Vol. vol. 2 (eds Ronald Spores & Robles García Nelly) 541-546 (Instituto Nacional de Antropología e Historia, 2014).

32 Acuna-Soto, R., Stahle, D. W., Cleaveland, M. K. & Therrell, M. D. Megadrought and megadeath in 16th century Mexico. *Emerg Infect Dis* **8**, 360-362 (2002).

33 Pickard, D. *et al.* Molecular characterization of the Salmonella enterica serovar Typhi Vi-typing bacteriophage E1. *Journal of bacteriology* **190**, 2580-2587, doi:10.1128/JB.01654-07 (2008).

34 Burbano, H. A. *et al.* Targeted Investigation of the Neandertal Genome by Array-Based Sequence Capture. *Science* **328**, 723-725, doi:10.1126/science.1188046 (2010).

35 Fu, Q. *et al.* DNA analysis of an early modern human from Tianyuan Cave, China. *Proceedings of the National Academy of Sciences of the United States of America* **110**, 2223-2227, doi:10.1073/pnas.1221359110 (2013).

36 Campbell, J. W., Morgan-Kiss, R. M. & Cronan, J. E., Jr. A new Escherichia coli metabolic competency: growth on fatty acids by a novel anaerobic beta-oxidation pathway. *Molecular microbiology* **47**, 793-805 (2003).

37 Rivera-Chavez, F. *et al.* Salmonella uses energy taxis to benefit from intestinal inflammation. *PLoS Pathog* **9**, e1003267, doi:10.1371/journal.ppat.1003267 (2013).

38 Liu, W. Q. *et al.* Salmonella paratyphi C: genetic divergence from Salmonella choleraesuis and pathogenic convergence with Salmonella typhi. *PLoS One* **4**, e4510, doi:10.1371/journal.pone.0004510 (2009).

39 Tam, C. K., Morris, C. & Hackett, J. The Salmonella enterica serovar Typhi type IVB self-association pili are detached from the bacterial cell by the PilV minor pilus proteins. *Infect Immun* **74**, 5414-5418, doi:10.1128/IAI.00172-06 (2006).

40 Tam, C. K., Hackett, J. & Morris, C. Salmonella enterica serovar Paratyphi C carries an inactive shufflon. *Infect Immun* **72**, 22-28 (2004).

41 Campana, M. G., Robles Garcia, N., Ruhli, F. J. & Tuross, N. False positives complicate ancient pathogen identifications using high-throughput shotgun sequencing. *BMC Res Notes* **7**, 111, doi:10.1186/1756-0500-7-111 (2014).

42 Wood, D. E. & Salzberg, S. L. Kraken: ultrafast metagenomic sequence classification using exact alignments. *Genome Biol* **15**, R46, doi:10.1186/gb-2014-15-3-r46 (2014).

43 Segata, N. *et al.* Metagenomic microbial community profiling using unique clade-specific marker genes. *Nat Methods* **9**, 811-814, doi:10.1038/nmeth.2066 (2012).

44 Singer, M. & Clair, S. Syndemics and public health: reconceptualizing disease in bio-social context. *Med Anthropol Q* **17**, 423-441 (2003).

45 Herring, D. A. & Sattenspiel, L. Social Contexts, Syndemics, and Infectious Disease in Northern Aboriginal Populations. *American Journal of Human Biology* **19**, 190-202, doi:10.1002/ajhb (2007).

46 Guy, P. L. Prospects for analyzing ancient RNA in preserved materials. *Wiley Interdiscip Rev RNA* **5**, 87-94, doi:10.1002/wrna.1199 (2014).

47 Gal-Mor, O., Boyle, E. C. & Grassl, G. A. Same species, different diseases: how and why typhoidal and non-typhoidal Salmonella enterica serovars differ. *Front Microbiol* **5**, 391, doi:10.3389/fmicb.2014.00391 (2014).

48 Wain, J., Hendriksen, R. S., Mikoleit, M. L., Keddy, K. H. & Ochiai, R. L. Typhoid fever. *Lancet* **385**, 1136-1145, doi:10.1016/S0140-6736(13)62708-7 (2015).

49 Monack, D. M., Mueller, A. & Falkow, S. Persistent bacterial infections: the interface of the pathogen and the host immune system. *Nat Rev Micro* **2**, 747-765 (2004).

50 Sahagún, B. d. *Florentine Codex: general history of the things of New Spain*. (1950-1982).

51 Zhou, Z. *et al.* Millennia of genomic stability within the invasive Para C Lineage of *Salmonella enterica*. *bioRxiv*, doi:10.1101/105759 (2017).

52 Achtman, M. *et al.* Multilocus sequence typing as a replacement for serotyping in Salmonella enterica. *PLoS Pathog* **8**, e1002776, doi:10.1371/journal.ppat.1002776 (2012).

53 Centers for Disease Control and Prevention (CDC). National Typhoid and Paratyphoid Fever Surveillance Annual Summary, 2014. (Atlanta, Georgia, 2016).
54 Acuna-Soto, R., Romero, L. C. & Maguire, J. H. Large epidemics of hemorrhagic fevers in Mexico 1545-1815. *Am J Trop Med Hyg* **62**, 733-739 (2000).
55 Smith, D. C. Gerhard's distinction between typhoid and typhus and its reception in America, 1833-1860. *Bull Hist Med* **54**, 368-385 (1980).
56 Crump, J. A., Luby, S. P. & Mintz, E. D. The global burden of typhoid fever. *Bull World Health Organ* **82**, 346-353 (2004).
57 World Health Organization. *Typhoid fever – Uganda*, <http://www.who.int/csr/don/17-march-2015-uganda/en/> (2015).
58 Burkhardt, S. & Kärkkäinen, J. in *Combinatorial Pattern Matching: 12th Annual Symposium, CPM 2001 Jerusalem, Israel, July 1–4, 2001 Proceedings* (ed Amihood Amir) 73-85 (Springer Berlin Heidelberg, 2001).
59 Ma, B., Tromp, J. & Li, M. PatternHunter: faster and more sensitive homology search. *Bioinformatics* **18**, 440-445 (2002).
60 Buchfink, B., Xie, C. & Huson, D. H. Fast and sensitive protein alignment using DIAMOND. *Nat Methods* **12**, 59-60, doi:10.1038/nmeth.3176 (2015).
61 Ning, Z., Cox, A. J. & Mullikin, J. C. SSAHA: a fast search method for large DNA databases. *Genome Res* **11**, 1725-1729, doi:10.1101/gr.194201 (2001).
62 Chao, K. M., Pearson, W. R. & Miller, W. Aligning two sequences within a specified diagonal band. *Comput Appl Biosci* **8**, 481-487 (1992).
63 Smith, T. F. & Waterman, M. S. Identification of common molecular subsequences. *J Mol Biol* **147**, 195-197 (1981).
64 Needleman, S. B. & Wunsch, C. D. A general method applicable to the search for similarities in the amino acid sequence of two proteins. *J Mol Biol* **48**, 443-453 (1970).
65 Benson, D. A. *et al.* GenBank. *Nucleic Acids Res* **41**, D36-42, doi:10.1093/nar/gks1195 (2013).
66 Dabney, J. *et al.* Complete mitochondrial genome sequence of a Middle Pleistocene cave bear reconstructed from ultrashort DNA fragments. *Proceedings of the National Academy of Sciences of the United States of America* **110**, 15758-15763, doi:10.1073/pnas.1314445110 (2013).
67 Meyer, M. & Kircher, M. Illumina sequencing library preparation for highly multiplexed target capture and sequencing. *Cold Spring Harb Protoc* **2010**, pdb prot5448, doi:10.1101/pdb.prot5448 (2010).
68 Kircher, M., Sawyer, S. & Meyer, M. Double indexing overcomes inaccuracies in multiplex sequencing on the Illumina platform. *Nucleic Acids Res* **40**, e3, doi:10.1093/nar/gkr771 (2012).
69 Briggs, A. W. *et al.* Removal of deaminated cytosines and detection of in vivo methylation in ancient DNA. *Nucleic Acids Res* **38**, e87, doi:10.1093/nar/gkp1163 (2010).
70 Hodges, E. *et al.* Hybrid selection of discrete genomic intervals on custom-designed microarrays for massively parallel sequencing. *Nat Protoc* **4**, 960-974, doi:10.1038/nprot.2009.68 (2009).
71 Tamura, K., Stecher, G., Peterson, D., Filipski, A. & Kumar, S. MEGA6: Molecular Evolutionary Genetics Analysis version 6.0. *Molecular biology and evolution* **30**, 2725-2729, doi:10.1093/molbev/mst197 (2013).
72 Stamatakis, A. RAxML version 8: a tool for phylogenetic analysis and post-analysis of large phylogenies. *Bioinformatics* **30**, 1312-1313, doi:10.1093/bioinformatics/btu033 (2014).
73 R Development Core Team. (The R Foundation for Statistical Computing, Vienna, Austria, 2011).
74 Connor, T. R. *et al.* What's in a Name? Species-Wide Whole-Genome Sequencing Resolves Invasive and Noninvasive Lineages of Salmonella enterica Serotype Paratyphi B. *MBio* **7**, doi:10.1128/mBio.00527-16 (2016).
75 Quinlan, A. R. & Hall, I. M. BEDTools: a flexible suite of utilities for comparing genomic features. *Bioinformatics* **26**, 841-842, doi:10.1093/bioinformatics/btq033 (2010).
76 Wickham, H. *ggplot2: Elegant Graphics for Data Analysis*. (Springer-Verlag New York, 2009).

Acknowledgements: This work was supported by the Max Planck Society (J.K.), the European Research Council (ERC) starting grant APGREID (to J.K.), Social Sciences and Humanities Research Council of Canada postdoctoral fellowship grant 756-2011-501 (to K.I.B.), and the Mäxi Foundation (M.G.C.). We thank the Archaeology Council at Mexico's National Institute of Anthropology and History (INAH) and the Teposcolula-Yucundaa Archaeological Project for sampling permissions. We are grateful to Antje Wissgott, Guido Brandt and Verena Schuenemann for assistance with laboratory work, Annette Günzel for providing graphic support, and Rodrigo Barquera, Jim Hackett and Menaka Pi for thoughts and discussion on the manuscript. Part of the data storage and analysis was performed on the computational resource bwGRiD Cluster Tübingen funded by the Ministry of Science, Research and the Arts Baden-Württemberg, and the Universities of the State of Baden-Württemberg, Germany, within the framework program bwHPC. We thank the MALT user community for helpful comments and bug reports.

Author Contributions: K.I.B., M.G.C., A.H., N.T. and J.K. conceived the investigation. K.I.B., A.H. Å.J.V., M.G.C. and J.K. designed experiments. N.M.R.G. provided archaeological information and drawings, submitted INAH permits and assisted in the sampling processes. Å.J.V., M.G.C., S.S., M.A.S. and K.I.B. performed laboratory work. Å.J.V., A.H., K.I.B., C.W. and A.A.V. performed analyses. D.H. implemented the MALT algorithm. A.H., J.K. and D.H. designed and set up the MALT ancient DNA analysis pipeline. C.W. performed ethnohistorical analyses. Å.J.V. and K.I.B. wrote the manuscript with contributions from all authors.

Competing financial interests: The authors declare no competing financial interests.

Figure 1 | Overview of Teposcolula-Yucundaa. A) Illustrates the location of the Teposcolula-Yucundaa site in the Mixteca Alta region of Oaxaca, Mexico; B) central administrative area of Teposcolula-Yucundaa showing the relative positioning of the Grand Plaza and churchyard cemetery sites. Burials within each cemetery are indicated with dark grey outlines and the excavation area is shaded in grey; C) drawing of individual 35 from which the Tepos_35 *S.* Paratyphi C genome was isolated. Panels B and C were adapted from drawings provided by the Teposcolula-Yucundaa archaeological project archives-INAH and ref. [30]. The figure was kindly provided by Annette Günzel.

Figure 2 | MALT analysis and pathogen screening of shotgun data. Shotgun data was analysed with MALT using a database constructed from all bacterial genomes available through NCBI RefSeq (December 2016). MALT results were visualized using MEGAN6[28]. The bar chart was constructed from the MEGAN6 output and is based on the per cent reads assigned to bacterial species when using a 95% identity filter. Reads assigned to *Salmonella enterica* are coloured red regardless. Other taxa to which 3% or more reads, per sample, were assigned are colour-coded depending on whether they are 'environmental' or 'human oral microbiome' bacteria. Remaining taxa are sorted into two categories: 'other environmental' or 'other microbiome' (Supplementary methods 3). Samples from the post-contact Grand Plaza epidemic cemetery containing *S. enterica* reads, contact era samples from the churchyard cemetery and the soil sample are illustrated. Additionally, a sample negative for *S. enterica* from the Grand Plaza cemetery (Tepos_27) is shown. Samples whose names are coloured in red are from the Grand Plaza and those in blue from the churchyard. The percentage of reads in the shotgun data assigned by MALT per sample is indicated at the top of each column. Only taxa with 4 or more reads assigned are visualized.

Figure 3 | Maximum Likelihood *S. enterica* phylogeny. Two maximum likelihood trees were produced. Positions with missing data were excluded in both cases. In panel a) the tree includes all five ancient genomes and is based on 3-fold SNP calls. It is based on 51,456 variant positions. b) shows a zoomed in view of the *S.* Paratyphi C genomes. In panel c) the tree includes two high-coverage ancient genomes and is based on 5-fold SNP calls. It is based on 81,474 variant positions. d) shows a zoomed in view of the *S.* Paratyphi C genomes, illustrating the branch shortening of the two ancient genomes (Tepos_14 and Tepos_35). Both trees were built with RAxML[72]. Branches coloured red indicate *S.* Paratyphi C genomes and branches in blue indicate other genomes that are human-specific and cause enteric (typhoid/paratyphoid) fever.

Table 1 | Overview of mapping statistics of captured sample libraries from the Grand Plaza (contact era) and churchyard (pre-contact)

Sample ID	Cemetery Site	Library treatment	# processed reads before mapping	# Unique mapped reads	Endogenous DNA (%) - quality filtered reads	Mean Fold Coverage	% of Genome Covered at least 3-fold
Tepos_10	Grand Plaza	non-UDG	16,945,834	399,561	20.56	4.35	52.17
		UDG	68,628,270	2,903,258	16.30	32.84	95.49
Tepos_14	Grand Plaza	non-UDG	20,559,478	1,222,402	23.51	14.41	95.77
		UDG	73,204,225	3,410,610	18.62	36.44	97.67
Tepos_35	Grand Plaza	non-UDG	27,248,720	1,803,043	31.37	25.50	97.67
		UDG	90,815,050	7,025,774	30.00	96.43	98.06
Tepos_11	Grand Plaza	non-UDG	21,941,119	19,576	0.87	0.21	0.93
		UDG	48,959,732	103,492	0.75	1.21	14.56
Tepos_20	Grand Plaza	non-UDG	771,431	15,236	6.94	0.15	0.26
		UDG	20,123,713	427,781	4.75	4.59	67.53
Tepos_34	Grand Plaza	non-UDG	18,934,710	123,307	2.55	1.35	14.65
		UDG	26,284,766	157,930	2.05	1.74	21.67
Tepos_36	Grand Plaza	non-UDG	23,147,904	36,224	0.75	0.40	1.76
		UDG	21,910,196	33,327	0.42	0.36	1.4
Tepos_37	Grand Plaza	non-UDG	5,223,138	218,874	9.28	2.55	42.12
		UDG	9,603,890	416,449	7.71	5.49	74.48
Tepos_38	Grand Plaza	non-UDG	8,280,412	18,308	0.91	0.19	0.97
		UDG	47,835,731	65,812	0.54	0.67	4.22
Tepos_41	Grand Plaza	non-UDG	17,608,445	33,664	0.72	0.37	1.47
		UDG	19,966,958	36,208	0.48	0.40	1.34
Tepos_27	Grand Plaza	non-UDG	17,931,300	4,778	0.07	0.04	0.27
Tepos_32	Churchyard	non-UDG	25,721,427	6,665	0.08	0.06	0.47
Tepos_43	Churchyard	non-UDG	31,129,662	3,426	0.05	0.03	0.25
Tepos_45	Churchyard	non-UDG	18,027,289	6,879	0.12	0.06	0.34
Tepos_48	Churchyard	non-UDG	17,915,341	4,312	0.06	0.04	0.25
Tepos_57	Churchyard	non-UDG	24,478,844	5,527	0.07	0.05	0.28
Soil	Grand Plaza & churchyard	non-UDG	10,875,300	796	0.02	0.01	0.07

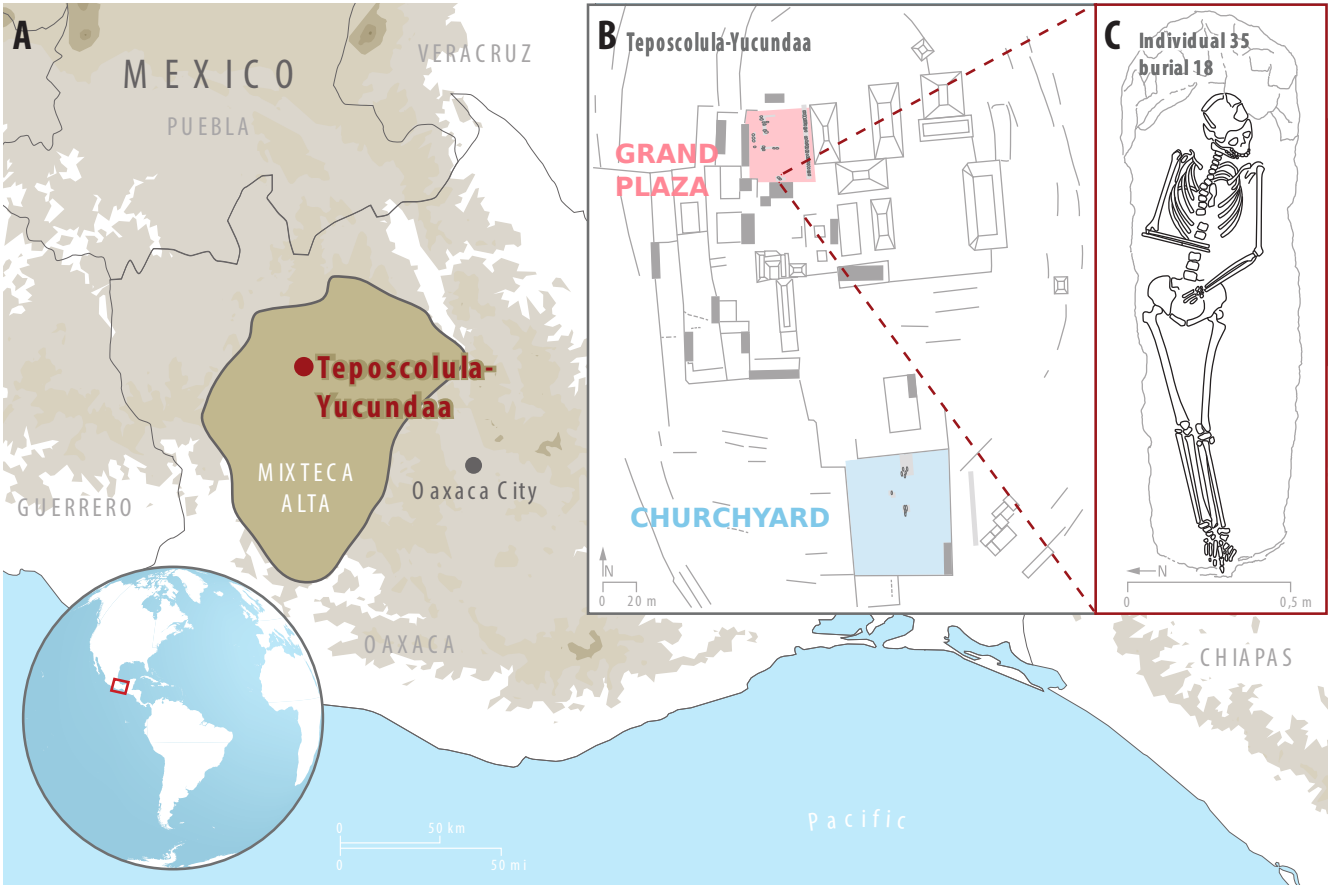
A
MEXICO
VERACRUZ
PUEBLA
Teposcolula-
Yucundaa
MIXTECA
ALTA
Oaxaca City
GUERRERO
OAXACA
CHIAPAS
Pacific
0 50 km
0 50 mi
B Teposcolula-Yucundaa
GRAND
PLAZA
CHURCHYARD
N
0 20 m
C Individual 35
burial 18
N
0 0,5 m

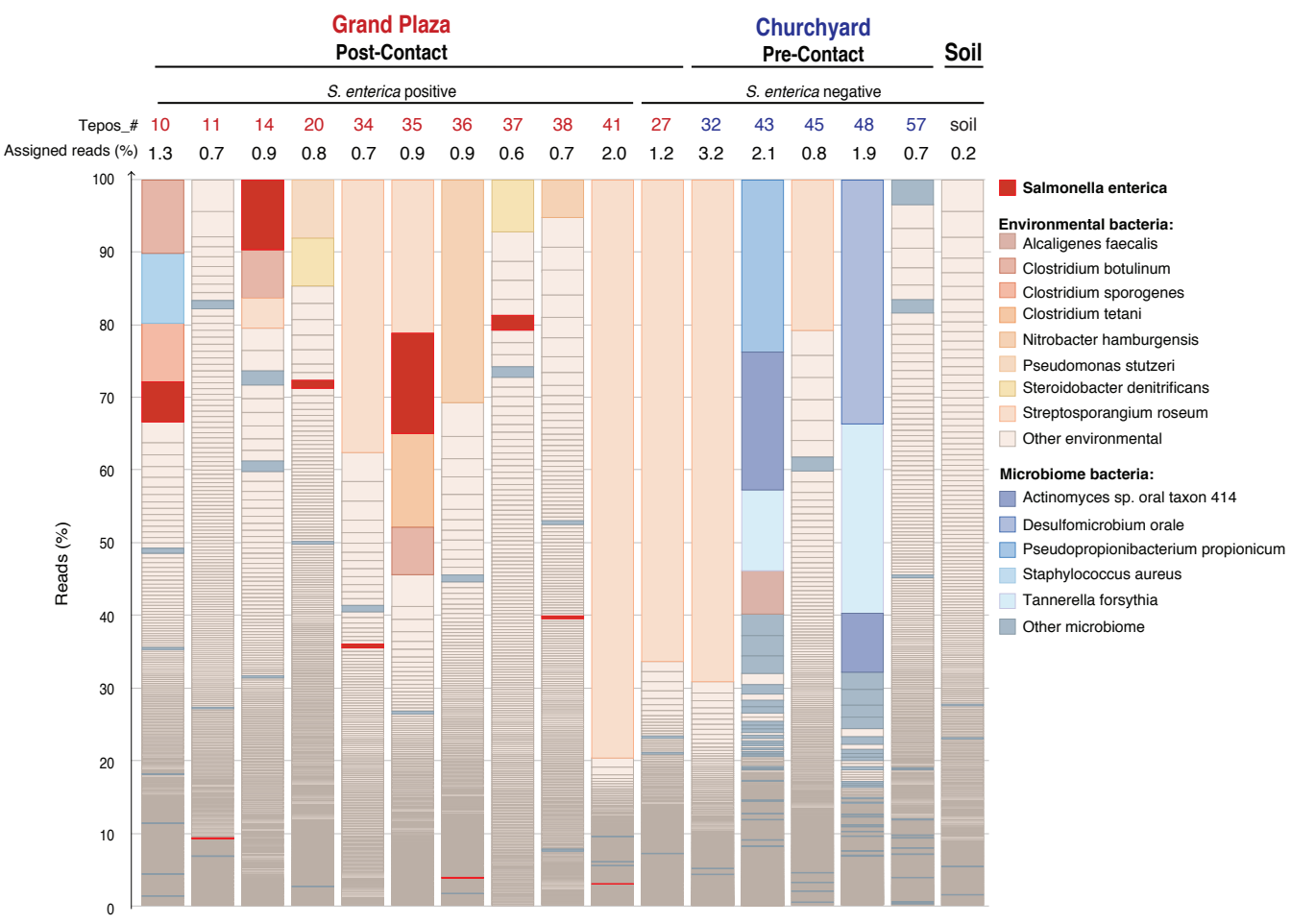
Grand Plaza
Post-Contact
Churchyard
Pre-Contact
Soil
S. enterica positive
S. enterica negative
Tepos_# 10 11 14 20 34 35 36 37 38 41 27 32 43 45 48 57 soil
Assigned reads (%) 1.3 0.7 0.9 0.8 0.7 0.9 0.9 0.6 0.7 2.0 1.2 3.2 2.1 0.8 1.9 0.7 0.2
Reads (%)
0
10
20
30
40
50
60
70
80
90
100
Salmonella enterica
Environmental bacteria:
Alcaligenes faecalis
Clostridium botulinum
Clostridium sporogenes
Clostridium tetani
Nitrobacter hamburgensis
Pseudomonas stutzeri
Steroidobacter denitrificans
Streptosporangium roseum
Other environmental
Microbiome bacteria:
Actinomyces sp. oral taxon 414
Desulfomicrobium orale
Pseudopropionibacterium propionicum
Staphylococcus aureus
Tannerella forsythia
Other microbiome

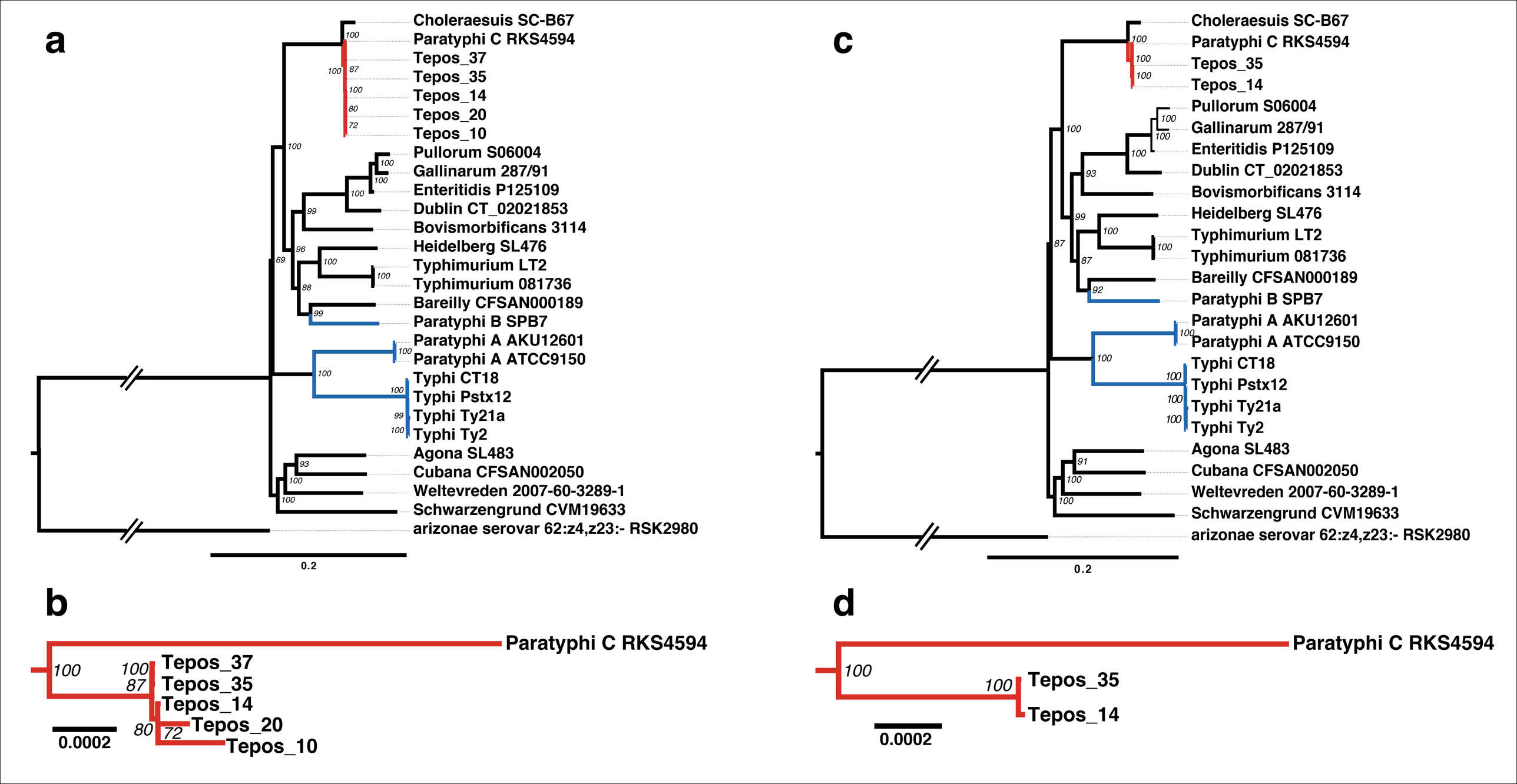
a
Choleraesuis SC-B67
Paratyphi C RKS4594
Tepos_37
Tepos_35
Tepos_14
Tepos_20
Tepos_10
Pullorum S06004
Gallinarum 287/91
Enteritidis P125109
Dublin CT_02021853
Bovismorbificans 3114
Heidelberg SL476
Typhimurium LT2
Typhimurium 081736
Bareilly CFSAN000189
Paratyphi B SPB7
Paratyphi A AKU12601
Paratyphi A ATCC9150
Typhi CT18
Typhi Pstx12
Typhi Ty21a
Typhi Ty2
Agona SL483
Cubana CFSAN002050
Weltevreden 2007-60-3289-1
Schwarzengrund CVM19633
arizonae serovar 62:z4,z23:- RSK2980
0.2
b
Paratyphi C RKS4594
Tepos_37
Tepos_35
Tepos_14
Tepos_20
Tepos_10
0.0002
c
Choleraesuis SC-B67
Paratyphi C RKS4594
Tepos_35
Tepos_14
Pullorum S06004
Gallinarum 287/91
Enteritidis P125109
Dublin CT_02021853
Bovismorbificans 3114
Heidelberg SL476
Typhimurium LT2
Typhimurium 081736
Bareilly CFSAN000189
Paratyphi B SPB7
Paratyphi A AKU12601
Paratyphi A ATCC9150
Typhi CT18
Typhi Pstx12
Typhi Ty21a
Typhi Ty2
Agona SL483
Cubana CFSAN002050
Weltevreden 2007-60-3289-1
Schwarzengrund CVM19633
arizonae serovar 62:z4,z23:- RSK2980
0.2
d
Paratyphi C RKS4594
Tepos_35
Tepos_14
0.0002